

1 **Title:** Survival analysis of wildlife cameras exposed to theft

2 **Authors:** Laura M. Cardona<sup>1\*</sup>, Barry W. Brook<sup>12</sup>, Zach Aandahl<sup>12</sup> and Jessie C. Buettel<sup>12</sup>

3

4 **Author's affiliations:**

5 <sup>1</sup> *School of Natural Sciences, University of Tasmania, Private Bag 55, Hobart, Tasmania*

6 *7001, Australia*

7 <sup>2</sup>*ARC Centre of Excellence for Australian Biodiversity and Heritage (CABAH), Australia*

8

9 **Author contributions**

10 **Laura M. Cardona:** Conceptualisation, Formal analysis, Methodology, Writing – original  
11 draft. **Barry W. Brook:** Conceptualisation, Methodology, Supervision, Writing – review &  
12 editing. **Zach Aandahl:** Conceptualisation, Formal analysis, Methodology, Writing – review  
13 & editing. **Jessie C. Buettel:** Conceptualisation, Methodology, Supervision, Writing –  
14 review and editing.

15 **Corresponding Author:**

16 \*Email: [laura.cardonaperez@utas.edu.au](mailto:laura.cardonaperez@utas.edu.au)

17 ORCID ID: <https://orcid.org/0000-0001-5328-8413>

18

19 **Co-author ORCID:**

20 Barry W. Brook: <https://orcid.org/0000-0002-2491-1517>

21 Zach Aandahl: <https://orcid.org/0000-0002-9412-8288>

22 Jessie C. Buettel: <https://orcid.org/0000-0001-6737-7468>

23 **Abstract**

24 Setting camera traps along roads is often necessary for ecological research, yet these  
25 locations expose cameras to theft leading to substantial data losses. Measures to minimise this  
26 risk include placing cameras away from human settlements. However, the effects of this and  
27 other measures on camera-trap theft risk are yet to be quantified. Here, we assessed the  
28 impact of gates on roads, the frequency of vehicle and human foot traffic, distance to the  
29 nearest town, and reduced visibility, on the risk of camera-trap theft, using a four-year,  
30 geographically extensive camera-trapping study in Tasmania, Australia. The large dataset  
31 covered 564 camera sites operating for 316,372 days (average of 561 camera days per unit),  
32 with 112 cumulative thefts. We used Bayesian survival modelling to determine the factors  
33 that best explained theft risk. Our results showed a high initial vulnerability to theft that  
34 gradually reduced over time, with significant predictors of reduced theft risk being: (i) road  
35 sites with lower frequencies of vehicle traffic, (ii) greater distance from the nearest town, (iii)  
36 where movement was curtailed by the presence of a gate, and (iv) a temporal trend that likely  
37 reflects a selective culling of ‘high exposure’ sites and increased efforts to hide camera units.  
38 The frequency of human foot traffic surprisingly did not significantly elevate theft risk. Our  
39 study provides important insights into the factors contributing to a higher risk of camera-trap  
40 theft on roads and offers a robust analytical framework to identify these factors for  
41 application in diverse social and ecological contexts.

42

43

44

45

46

## 47 **Introduction**

48 Camera traps (CTs) have become an increasingly effective tool in ecological research and for  
49 monitoring human activity for park management (Burton *et al.* 2015; Miller *et al.* 2017;  
50 Cardona *et al.* 2024). Their applications have included estimating wildlife abundance (e.g.,  
51 Taylor *et al.* (2022)), population dynamics (e.g., Karanth *et al.* (2006)), and human and  
52 wildlife activity patterns (e.g., Miller *et al.* (2017)). While their use continues to increase, the  
53 risk of theft of such devices remains one of the major constraints on their effectiveness  
54 (Glover-Kapfer *et al.* 2019). Camera-trap theft can lead to substantial costs, and result in  
55 significant loss of data, disruption of long-term studies, unequal sampling across study sites  
56 and seasons, bias in sampling protocols, and variation in sampling effort (Kukielka *et al.*  
57 2013; Paula *et al.* 2015; Pyšková *et al.* 2018; Meek *et al.* 2019).

58

59 Researchers using CTs face the dual challenge of preventing data loss due to theft, while  
60 ensuring cameras are appropriately placed for optimal data collection (Cusack *et al.* 2015;  
61 Meek *et al.* 2019). The strategy used to determine camera locations, including their  
62 placement on or off roads, influences the detection probability of wildlife species and is  
63 crucial for obtaining unbiased estimates of species richness, abundance, activity, and  
64 subsequent monitoring (Cusack *et al.* 2015; Mann *et al.* 2015; Tanwar *et al.* 2021). While  
65 placing CTs at sites away from human presence, such as random forest sites and animal trails,  
66 reduces the risk of theft, setting them on man-made features, such as roads, is ideal for  
67 monitoring the activity of many species that prefer or are more readily detected on these  
68 features, such as carnivorous, cryptic, and introduced species (Cusack *et al.* 2015; Mann *et al.*  
69 2015; Iannarilli *et al.* 2021). Moreover, cameras set on roads can indirectly capture human  
70 activity, which can be important information for land management (Miller *et al.* 2017;

71 Cardona *et al.* 2024). Additionally, in regions difficult to access, these features are often the  
72 only feasible locations to deploy CTs (Meek *et al.* 2014). As a result, placing CTs on roads is  
73 crucial for enhancing our understanding of predator-prey dynamics, human-wildlife  
74 interactions, and visitor behaviour in protected areas. However, the ongoing risk of theft,  
75 often forces researchers into a trade-off that leads them to prioritise less-vulnerable but lower-  
76 animal-activity locations off roads (e.g., Hossain *et al.* (2016)), impacting the study  
77 objectives and outcomes.

78

79 As such, over the past decades, diverse strategies to protect CTs deployed on roads from theft  
80 have been proposed and attempted in the literature. These include physically securing CTs by  
81 mounting them on security posts or locking them to trees with braided steel cables and  
82 padlocks (Kelly *et al.* 2008; Meek *et al.* 2012a), as well as deterring and reducing their  
83 exposure to thieves by attaching warning messages (Clarín *et al.* 2014; Meek *et al.* 2019) and  
84 limiting the duration that CTs remain deployed in the field (e.g., Wegge *et al.* (2004); Glen *et*  
85 *al.* (2013)). Other strategies involve conducting surveys during times of the year or the day  
86 when human activity is less frequent at survey sites (e.g., early mornings or off-peak tourism  
87 seasons), positioning CTs far from human settlements (e.g., Rovero *et al.* (2009)), and  
88 camouflaging cameras with bark and leaves (e.g., Hossain *et al.* (2016); Zahoor *et al.* (2023)).  
89 While the effectiveness of measures such as using personal messages and security posts to  
90 minimise theft incidents has been tested (Meek *et al.* 2012a; Clarín *et al.* 2014), the effect of  
91 factors, such as the distance of the CT to human settlements, on the risk of camera-trap theft  
92 remains debated and has not yet been quantified rigorously.

93 In this study, we analysed a pre-existing data set that includes many theft occurrences from a  
94 four-year wildlife monitoring project in diverse regions of Tasmania, Australia. Across the

95 four-year period, a cumulative total of 20% of CTs deployed on a mix of forestry, dirt and  
96 gravel roads were stolen (Figure. 1). Using these data, we aimed to investigate the extent to  
97 which the proximity of the CT to the nearest town, the frequency of vehicle and human foot  
98 traffic at the camera site, the presence of gates on roads, and the researchers' growing  
99 expertise in hiding CTs from potential thieves (e.g., improving camouflage and prioritising  
100 infra-red flash cameras), influenced the risk of camera-trap theft. By doing so, our goal was  
101 to identify factors driving the risk of camera-trap theft and contribute to the development of  
102 targeted strategies that enhance the protection of CTs.



103

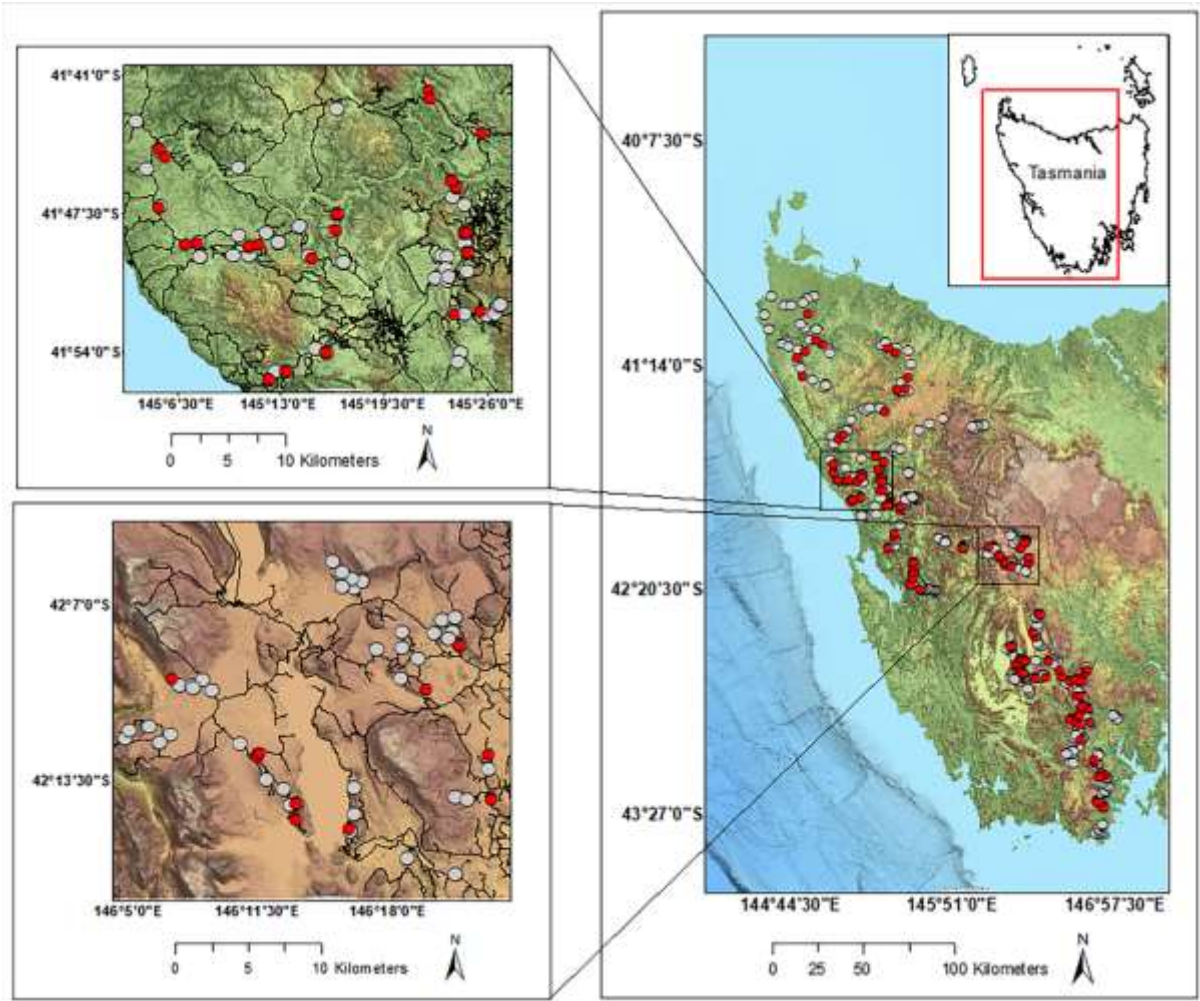
104 **Figure 1.** Example of a site where a camera trap was stolen during the 4-year camera-trap  
105 monitoring project in Tasmania, Australia.

106 **Materials and Methods:**

107 **Camera trap dataset and number of stolen cameras**

108 We used data on camera trap (CT) theft occurrences sourced from the Dynamics of Eco-  
109 evolutionary Patterns (D.E.E.P) group, University of Tasmania, remote wildlife monitoring  
110 program (Vaughan *et al.* 2022; Paton *et al.* 2024). The camera-trap network was distributed  
111 across the southeastern, central highlands, northwestern and western regions of Tasmania,  
112 Australia (Figure 2). These regions encompass a diversity of vegetation communities,  
113 including dry and wet sclerophyll forests, temperate rainforests, low heaths, shrublands, and  
114 open buttongrass moorlands, as well as a wide range of land uses such as parks and reserves,  
115 production forests (logging), and private lands. The study area is crisscrossed by highways  
116 and smaller roads, including numerous dirt or gravel roads commonly used during the day by  
117 vehicles and walkers, with nighttime human activity infrequent. These regions cover a broad  
118 gradient of development and varying levels of human activity.





119

120

**Figure 2.** Map of the study area and the location of the camera trap sites. The different

121

colours show whether the camera was stolen (red) or not stolen (grey). The insets show two

122

examples of the camera-network deployments at finer spatial scales.

123

124

The monitoring network involved 564 camera sites, using a standard model (Cuddeback X-

125

Change model 1279, which have a changeable flash unit), placed 100 m or greater apart and

126

positioned on a mix of forestry, dirt and gravel roads. The network was operational for a total

127

of 316,372 camera days (minimum estimation, as this does not include those service periods

128

with thefts) between June 2018 to March 2022; 357 CTs were initially deployed in 2018 and

129

an additional 207 CT sites rolled out over 2019 to 2021. The CTs were unbaited, mounted on

130

trees on average 30 cm off the ground adjusted to target medium-large mammal species, and

131 equipped with either an infrared flash or white flash. Infra-red cameras were programmed  
132 with 30 s delay for both day and night, while white flash units operated with 30 s delay  
133 during the day and one min at night. CTs were serviced every 4-6 months to download  
134 images, replace batteries, remove vegetation obstructing the field of view. In cases where a  
135 camera was stolen, a new CT was deployed at a new site, typically >250m from the stolen  
136 camera's location.

137

138 All CTs were camouflaged with vegetation upon their deployment. However, after  
139 researchers experienced thefts of CTs deployed during the first year (2018), they intensified  
140 their camouflage techniques in subsequent years to better conceal the CTs from view. This  
141 enhanced approach included carefully selecting sites with natural vegetation cover,  
142 conducting thorough visual inspections from various points before finalising the setup, and  
143 regularly replacing the vegetation used for camouflage during the following service checks.

144 Across the four-year period a total of 112 CTs, or 20% of all those deployed, were eventually  
145 stolen (although the lifetime of a given camera at a site varied considerably): 14 cameras in  
146 2018, 38 in 2019, 30 in 2020, 23 in 2021, and seven in 2022 (Figure 2). While the year a CT  
147 was stolen was known, the exact date remained unknown, as researchers only discovered a  
148 unit was missing during servicing visits meaning a CT could have been stolen at any point  
149 since the last service check. Since the exact date a CT was stolen was unknown, we chose to  
150 use a Bayesian survival analysis, to investigate the impact of the various predictors on the  
151 risk of camera-trap theft. This allowed us to include general interval-censored data under the  
152 proportional hazards model and thereby account for uncertainties surrounding the exact  
153 moment of camera-trap theft (see Section *Bayesian Survival analysis of camera-trap theft* for  
154 details).



155

156 **Statistical analysis**

157 **Model covariates - Predictors of theft.**

158 We tested survival models using five predictors: distance to the nearest town, gates on roads,  
159 the frequency of vehicle and human foot traffic at the site, and the researchers' growing  
160 expertise in hiding cameras from potential thieves, as detailed below:

161

162 a) The distance from each CT site to the nearest town with permanent residents (Appendix  
163 S1: Table S1) was calculated as the Great Circle Distance, in kilometres, using Google Earth  
164 satellite images. To account for variance heterogeneity, this distance was normalised by  
165 subtracting the mean and dividing by the standard deviation (SD) prior to analysis. The  
166 presence of a gate on the roads (e.g., forestry gates, National Park gates, and residential gates)  
167 was defined as a binary covariate where 0 = no gate, and 1 = presence of a gate.

168

169 b) The frequency of vehicle and human foot traffic at the CT site was expressed as an index  
170 of relative activity (RA). This index was estimated for each CT site by calculating the number  
171 of images of 'vehicles' (e.g., all-terrain vehicles, motorbikes, bicycles, forestry vehicles, and  
172 two-wheel drives) and/or 'humans on-foot' (e.g., hikers, joggers, or people with dogs)  
173 divided by the number of active trap days at that station (George *et al.* 2006). We added one  
174 to this RA to allow the inclusion of zero values (sites with only vehicle or human-foot traffic)  
175 and because the researchers at a minimum had visited the sites, and then log-transformed this  
176 value before analysis to account for heterogeneity of variances:  $\log(RA + 1)$ . The  
177 categorisation into 'vehicle' or 'human on-foot' of the large dataset of images was done using

178 the freely available object detection software MegaDetector (Beery *et al.* 2019; Brook *et al.*  
179 2023). We were not able to calculate the index of RA for CTs stolen within the first four-six  
180 months of their deployment which was before their first service check (n=42 cameras), as no  
181 data was ever retrieved from these cameras before being stolen. Since using these missing  
182 values or excluding these cameras from the subsequent analysis could have impacted the  
183 conclusions drawn from the model selection (Donders *et al.* 2006; Nakagawa *et al.* 2011) or  
184 result in reduced estimation precision or statistical power (Nakagawa *et al.* 2011), especially  
185 because they were likely to be highly vulnerable sites, we imputed the missing values. As the  
186 data was Missing Not At Random—since the missing variable (number of images of vehicles  
187 and/or humans on-foot) was directly tied to the dependent variable (being stolen) (Nakagawa  
188 *et al.* 2011)—we imputed the missing data by generating random values based on a Gaussian  
189 probability distribution. The mean was defined as the RA of the closest CT located at least 2  
190 km away, and the standard deviation was set at 10% of the confidence interval. Two cameras  
191 did not have a CT at least 2km away and were therefore excluded from the subsequent  
192 analysis.

193

194 c) The predictor ‘deployment expertise’ was included to account for potential biases arising  
195 from adaptive changes to the deployment strategies used by the researchers to reduce the  
196 visibility of CTs. We categorised this predictor into ‘initial deployment’ referring to the first  
197 CTs deployed by researchers during the year 2018, and ‘informed deployment’ referring to  
198 CTs deployed in subsequent years (from 2019 to 2022). In 2018, both the rates and causes of  
199 camera-trap theft in these regions of Tasmania were unknown by the researchers, and  
200 avoiding theft of such devices was not considered a high priority. However, during the  
201 subsequent years (from 2019 to 2022), given the large number of stolen CTs during 2018,  
202 researchers increasingly focused on implementing strategies to reduce the visibility of CTs by

203 potential thieves. These strategies included selectively culling sites that were highly exposed  
204 and easily discovered by thieves, based on previous incidents of camera-trap theft at those  
205 sites; greater emphasis on improving the camouflage of CTs; and the situational prioritisation  
206 of CTs with infra-red rather than white-bulb flash.

207 All the predictors had a Pearson's cross-correlation coefficient  $r < 0.7$ .

208

### 209 **Bayesian Survival analysis of camera-trap theft**

210 All analyses were done using R version 4.2.2 (R Core Team 2020). To investigate the impact  
211 of the various predictors on the risk of camera-trap theft we used survival analysis within a  
212 Bayesian framework using the package '*rstanarm*' (Brilleman *et al.* 2020). We chose to  
213 use Bayesian survival analysis (parametric) because our study incorporates interval-censored  
214 data as the exact date a CT was stolen is unknown, but it falls within a known interval—  
215 between two consecutive CT service sessions. Although the Cox proportional hazards model  
216 has been the most widely used semiparametric regression model in the survival literature, its  
217 partial likelihood method is not applicable for interval-censored data under this model (Lin *et*  
218 *al.* 2015; Brilleman *et al.* 2020). As such, a Bayesian approach offers an efficient approach  
219 for analysing interval-censored data under the proportional hazards model, and properly  
220 accounts for uncertainties surrounding the exact time of camera-trap theft. This model  
221 characterised the censored data as a series of intervals  $[L_i, R_i]$  for each subject  $i$ , where  $L_i$  and  
222  $R_i$  denote the left and right end of the interval within which the theft of a CT was known to  
223 have occurred (Pan *et al.* 2020), specifically between two consecutive service sessions of the  
224 CT. For CTs that were not stolen and were removed on a known date, both  $L$  and  $R$  were set  
225 equal, thus representing the exact number of days the camera remained in the field until its  
226 removal.

227

## 228 **Covariate analysis with model comparison**

229 To check the appropriateness and robustness of the Bayesian survival analysis, we first  
230 identified and selected the parametric model that best fit our data. To do this, we compared 14  
231 different models, each comprising a saturated survival model paired with various parametric  
232 baseline hazard functions (Weibull, exponential, basis spline and monotone spline, that latter  
233 two with different degrees of freedom). To assess how well the assumptions of the best-fitting  
234 parametric model aligned with the actual data and identify potential discrepancies, we  
235 compared that model's predicted survival function using the *Posterior\_survfit* method for  
236 'stansurv' objects, against Kaplan Meier survival curve estimates using R package 'survival'  
237 (Therneau 2020). We visualised results from the Kaplan Meier survival curve estimates  
238 using the R package 'survminer' (Kassambara *et al.* 2021). Given that the Kaplan-Meier  
239 method is only suited for right-censored data, we calculate the median number of days within  
240 each time interval and used it as an estimate of the censored days (approximate days in the field  
241 before the CT was stolen).

242

243 Once we selected the best fitting parametric form of the hazard function on the saturated  
244 model, we used it to fit and compare all possible simpler linear combinations of the five  
245 predictors, resulting in 32 candidate models. For the best-fitting model, we estimated the  
246 posterior distribution of the model parameters using a Bayesian estimation via Markov Chain  
247 Monte Carlo (MCMC). Variables with 95% credible intervals (CI) not overlapping with 0  
248 were considered to have strong evidence for effects on camera-trap theft. If the 95% CI did  
249 not overlap with 0 and the limits were negative, we could be 95% confident that the mean of  
250 the intervention group would on average, lie within negative values and present a lower mean

251 compared to the comparison group. Predictions were visualised using the *posterior\_survfit*  
252 function, which provides survival probability estimates along with their lower (10%) and  
253 upper (90%) credible intervals for every possible combination of predictor values at each  
254 time point. Predictions were made considering the upper (0.95%) and lower (0.05%) quantile  
255 values for continuous covariates and both levels for the categorical (binary) covariates.

256

257 For each model we used sufficient iterations to ensure convergence (typically ~ 2,000  
258 iterations) (van de Schoot *et al.* 2021). To establish chain convergence, we used the R-hat  
259 diagnostic (R-hat <1.01). Model selection was done using leave-one-out (LOO) cross  
260 validation, which assesses the predictive performance of models in a Bayesian setting by  
261 estimating the information-theoretic, relative expected Kullback-Leibler discrepancy (Yates  
262 *et al.* 2023). The best model was selected based on the expected log predictive density values  
263 (scores) and expert knowledge.

264

## 265 **Results**

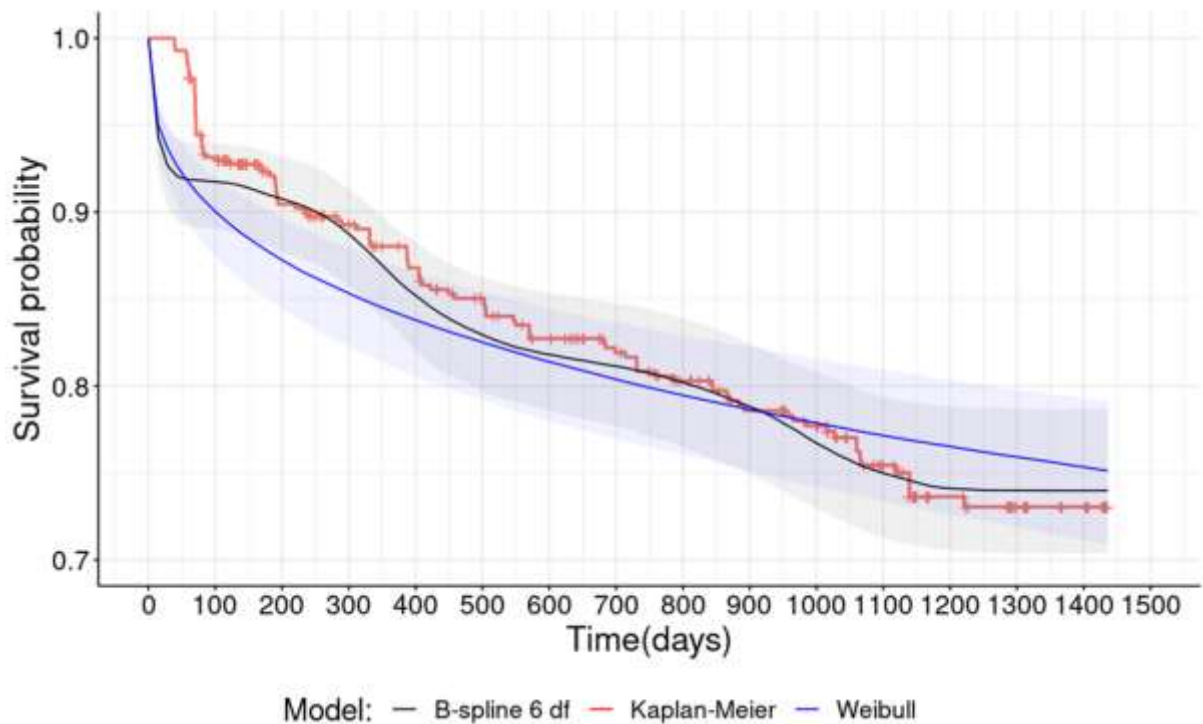
### 266 **Parametric form of the hazard function.**

267 The Weibull model was the best fitting parametric form of the hazard function for our data set  
268 followed by the Basis spline model with the highest degree of freedom as internal knots (six  
269 degrees of freedom) (Appendix S1: Figure S1). The Weibull model slightly over-estimated  
270 the Kaplan-Meier estimates during the initial period of 0 to 900 days and slightly  
271 underestimated them in the later period from 900 to 1436 days. The second-best-fitting  
272 model implied a higher degree of flexibility closely approaching to the Kaplan-Meier curve.  
273 However, this flexibility may lead to overfitting the current dataset which could reduce the  
274 model's predictive accuracy on new data (Figure 3).

275

276 The Weibull curve modelling the predicted risk of camera trap (CT) theft was characterised  
277 by a shape parameter less than 1 ( $k = 0.4$ ), suggesting theft rates of CTs were higher shortly  
278 after their deployment, with this rate thereafter decreasing over time (Figure 3).

279



280

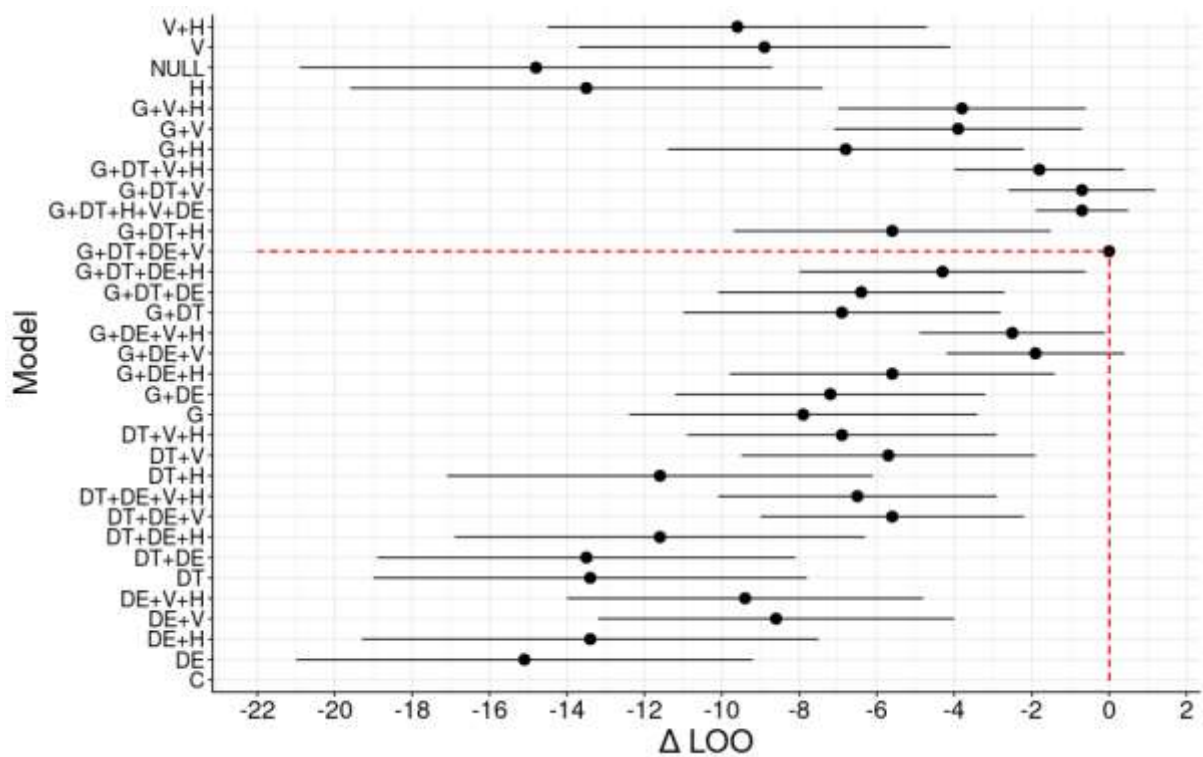
281 **Figure 3.** Predicted survival probability of camera traps over time using the best fitted  
282 parametric form of the hazard function; Weibull survival model (posterior median and 95%  
283 uncertainty limits), the second best fitting parametric form; B-spline survival model with 6  
284 degrees of freedom (df) (posterior median and 95% uncertainty limits), and the non-  
285 parametric Kaplan-Meier hazard estimate.

286

287 **Covariate analysis with model comparison using the Weibull hazard function.**

288 The model containing the predictors ‘deployment expertise’, ‘distance to town’, ‘vehicle  
 289 relative activity’ (RA) and ‘gate presence’ had the best predictive performance on the survival  
 290 of CTs (Figure 4). This suggested that human on-foot RA was not as important as the other  
 291 four covariates in explaining the variance in camera-trap theft in our context. The simpler  
 292 models, each of which pool estimates for at least one of the covariates, performed poorly  
 293 relative to the best-performing models (Figure 4, Appendix S1: Table S2).

294



295

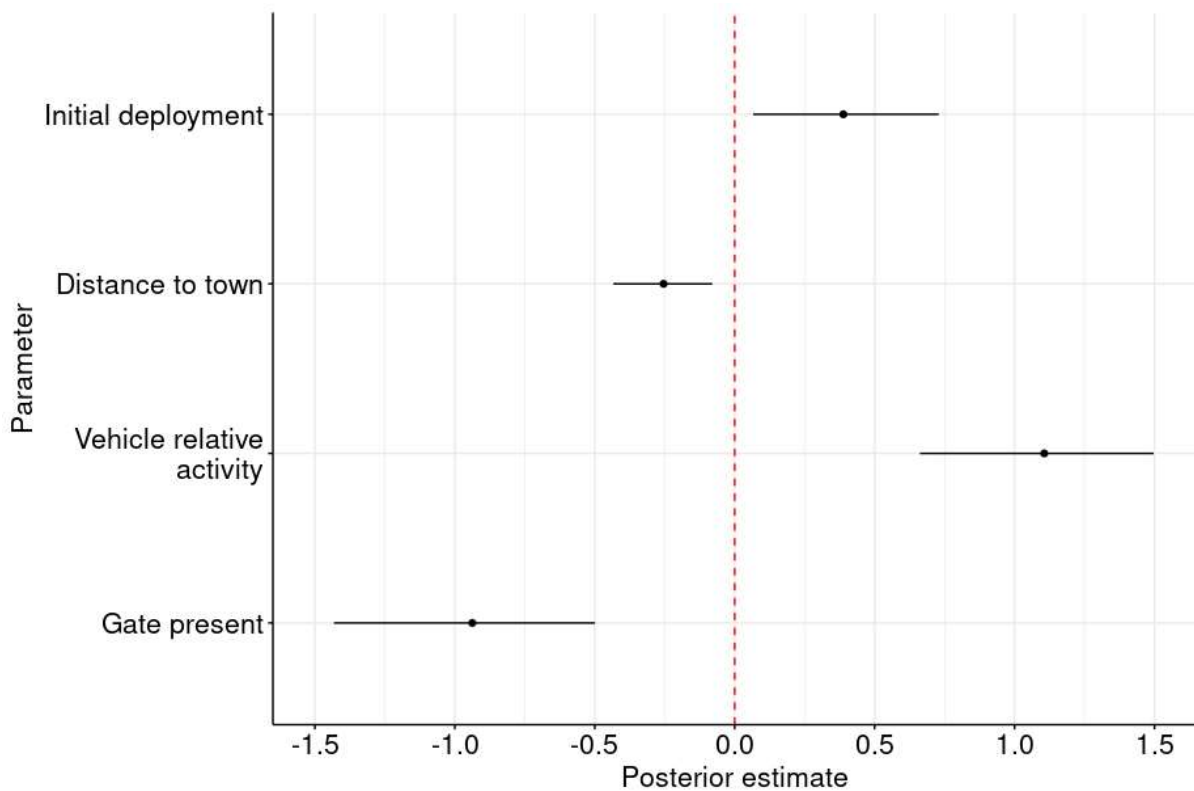
296 **Figure 4.** Estimates of model performance using approximate leave-one-out cross-validation.

297 The scores  $\Delta LOO_i = LOO_i - LOO_{min}$  are the differences of the loo estimates of  
 298 models  $i = 1, \dots, 32$  and that of lowest LOO value. The error bars depict one-standard error  
 299 of the  $\Delta LOO_i$  estimates. G = Gate presence, DT = Distance to town, DE = Deployment  
 300 expertise, H = Human on-foot relative activity, V = vehicle relative activity.

301



302 All predictors included in the best-fitting model showed strong evidence for their impact on  
 303 CT survival probability, as their parameter posterior estimates and 95% Bayesian credible  
 304 intervals did not overlap with 0 (Figure 5). Distance to town and deployment expertise had  
 305 the lowest posterior estimates. Increasing distance to town and gate presence lead to a  
 306 decrease in the hazard function by approximately 25.9% and a 59.3% respectively.  
 307 Conversely, an increase in one unit of the log-transformed vehicle RA and initial deployment  
 308 showed evidence of increasing the hazard function by approximately 200.4% and 49.2%  
 309 respectively.

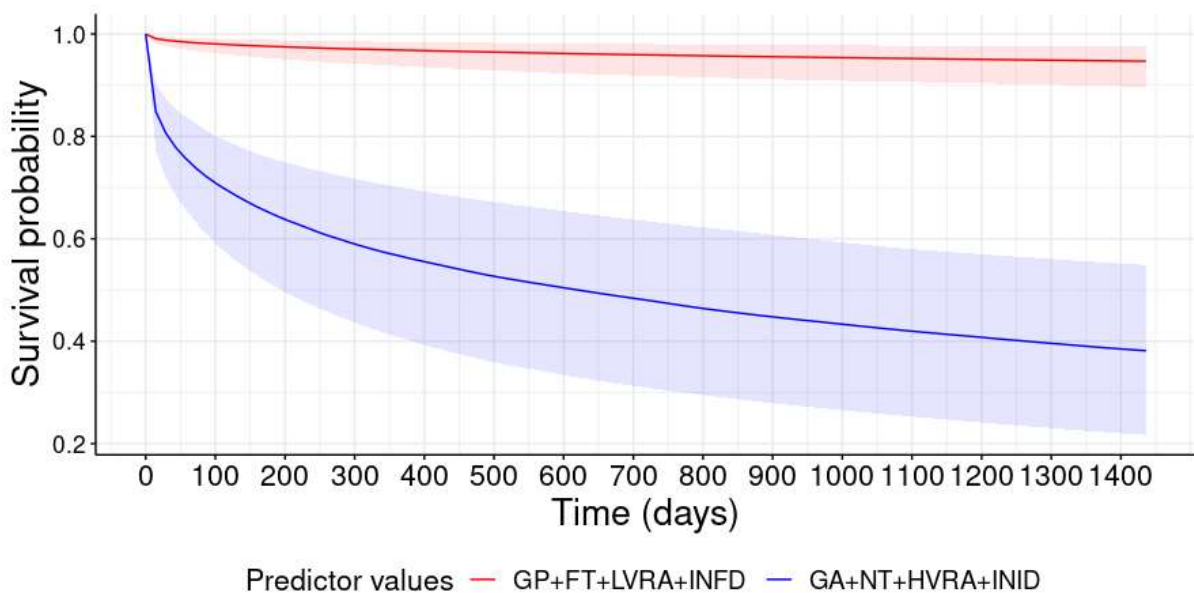


310  
 311 **Figure 5.** Parameter posterior estimates of predictors included in the best-fitting model (see  
 312 Figure 4). Horizontal lines indicate 95% Bayesian credible intervals on camera survival  
 313 probability; the intervals do not overlap with 0 (vertical red line) indicating a strong effect on  
 314 camera-trap theft.

315

316 The predictions of our best model showed that informed deployment, the presence of a gate  
 317 on the road, a decrease in vehicle RA (lowest 5% quantile = 0.049 images of vehicles per  
 318 total trap days), and greater distance from the nearest town (highest 95% quantile = 32 km)  
 319 significantly increased the survival probability of CTs (Figure 6). These CTs were predicted  
 320 to last 205 times longer without being stolen compared to cameras situated in the worst  
 321 circumstance: closer to the nearest town (lowest 5% quantile = 5km), on roads without a gate,  
 322 higher vehicle RA (highest 95% quantile = 0.980 images of vehicles per total trap days), and  
 323 initially deployed (Figure 6).

324



325

326 **Figure 6.** Predicted survival probability of camera traps over time (posterior median and 95%  
 327 uncertainty limits) under the best- (red) and worst-case (blue) combinations of parameter  
 328 values. LVRA = lowest vehicle relative activity (5% quantile = 0.049 vehicle images of  
 329 vehicles per total trap days), HVRA = highest vehicle relative activity (95% quantile = 0.980  
 330 of vehicles per total trap days), FT = Furthest distance from the nearest town (95% quantile =  
 331 32 km), NT = nearest distance to the nearest town (5% quantile = 5 km), GP = gate on road  
 332 present, GA = gate on road absent, INFD = informed deployment, INID = initial deployment.

333 **Discussion**

334 In this study, we assessed the impact of a range of factors related to camera trap (CT)  
335 placement on the risk of theft of CTs deployed on roads. Interestingly, we found that the  
336 frequency of human foot traffic was not a significant factor in camera-trap theft prevention.  
337 However, a decrease in the frequency of vehicle traffic, the presence of gates on roads, longer  
338 distances to towns, and increasing experience at hiding cameras all showed evidence of  
339 significantly decreasing camera-trap theft risk.

340

341 Although the exact motivations behind why people steal CTs remains unclear, it is likely that  
342 individuals engaging in illegal activities would steal CTs to avoid being identified, and sites  
343 with these characteristics in our study were less frequented by such individuals. Gated roads  
344 clearly have limited vehicle access, and this will reduce the likelihood of illicit activity such  
345 as illegal forest extraction and hunting, as vehicles facilitate rapid ingress and egress from  
346 sites, and the transportation of tools (e.g., chainsaws, axes and hunting gear), and recovery of  
347 materials associated with such activities (e.g., wood and carcasses) (Clements *et al.* 2014;  
348 Woods 2019). In contrast, individuals on foot are generally more likely involved in  
349 recreational activities like walking dogs, hiking and jogging. This is consistent with our  
350 results, which showed that while the frequency of vehicle traffic was a significant predictor of  
351 camera-trap theft, the frequency of human foot traffic was not.

352

353 Secondly, locked gates might foster a perception of increased risk among potential offenders  
354 of getting caught or facing consequences, as demonstrated in urban settings like alleys  
355 (Sidebottom *et al.* 2018). This perception could deter unauthorised individuals, such as  
356 motorbikes that can bypass gates, from using these roads for illegal activities. However, the

357 effectiveness of gates in creating a fear of prosecution in remote areas depends on whether  
358 managers have the resources to monitor and enforce laws in the area (Abdu 2023). Therefore,  
359 in areas lacking adequate monitoring against crime, the presence of a gate on the road might  
360 no longer be a strong determinant of the risk of camera-trap theft. Additionally, the frequency  
361 of vehicles like motorbikes and bicycles might impact this risk differently compared to other  
362 vehicles that cannot bypass gates, such as large four-wheel drives. Advances in machine-  
363 learning models for identifying different types of vehicles in CT images, like MegaDetector  
364 (Beery *et al.* 2019), could help future studies examine the impacts of specific types of  
365 vehicles on camera-trap theft on roads with and without a gate.

366

367 Proximity to the nearest town likely attracts more individuals engaged in illegal activities,  
368 such as vandals and opportunistic thieves, as these roads require less effort and time to reach.  
369 Previous studies have found that forests and farms near towns experience higher instances of  
370 illegal forest extraction, vandalism, unauthorised trespassing, and illegal hunting (Barclay *et al.*  
371 *al.* 2011; Mackenzie *et al.* 2013). However, crime and illegal activity in these areas are not  
372 solely determined by their proximity to towns but also by the socioeconomic status,  
373 educational levels, and social dynamics of nearby communities, as well as the ecology of the  
374 area, such as resource availability and canopy cover (Gerben J. N. Bruinsma 2007; Troy *et al.*  
375 2012; Mackenzie *et al.* 2013; Abdu 2023). Therefore, in areas with, for example, stronger  
376 community social cohesion, roads near towns might have low or no levels of illegal activity,  
377 potentially leading to no correlation between distance to town and camera-trap theft risk, as  
378 suggested in previous studies (Meek *et al.* 2019).

379

380 As researchers work within and become familiar with the broad risks associated with a given  
381 operational region, they inevitably improved the measures used to hide CTs from potential  
382 thieves. Our results showed that this significantly reduced camera-trap theft risk, likely  
383 because better-hidden CTs were harder for potential thieves to detect, and because the most  
384 vulnerable sites were quickly plundered and thereafter abandoned. These findings emphasise  
385 the importance of using strategies such as enhance camouflage and prioritising infra-red flash  
386 to mask CTs and minimise their visibility to people. However, the separate impact of  
387 camouflaging CTs and using infra-red flash on camera-trap theft risk warrants further  
388 investigation. A future study could include a controlled experiment comparing the effects of  
389 camouflaged and non-camouflaged CTs on the risk of camera-trap theft using dummy units.  
390 Another study could involve collaborating with researchers who deployed both infra-red and  
391 white flash CTs on roads with consistent nighttime human activity and experienced theft.  
392 Moreover, there are unfortunately trade-offs in these choices. While infra-red flashes are less  
393 noticeable to people during nighttime, they produce monochrome images, compared to the  
394 bright and coloured images of white-flash cameras (Meek *et al.* 2012b). Infra-red flash  
395 images also reduce the detection and identifiability of certain small mammals, as well as  
396 species that rely on pelage colour as an identifying characteristic (Meek *et al.* 2015; Burns *et*  
397 *al.* 2018). Another risk – data quality trade-off involves site obscuration: if not arranged  
398 correctly, the vegetation used for camouflaging CTs can obstruct the cameras field-of-view,  
399 leading to poor image quality, empty frames, or misleading clutter that resembles animals  
400 (Moll *et al.* 2020).

401

402

403

404 **Conclusion**

405 The evidence from this study suggests that placing CTs on roads with a gate, at greater  
406 distance from the nearest town, and with lower frequencies of vehicle traffic, as well as  
407 implementing proactive efforts to hide CTs, reduces theft risk. It is interesting to note that  
408 human foot traffic did not significantly elevate this risk in our context, suggesting that the  
409 influence of the frequency of human activity on the risk of CT theft depends on the type of  
410 activity. To our knowledge, these effects have not been rigorously quantified before, but  
411 further data are needed from other social and ecological contexts. Our study offers a robust  
412 analytical framework for identifying and testing the factors influencing CT theft risk with  
413 application in diverse social and ecological contexts. Moreover, these results indicate that to  
414 enhance security of CTs deployed on roads, efforts must go towards multiple anti-theft  
415 measures, including strategic placement based on the social and ecological landscape and  
416 proactive efforts to hide cameras. If resources are limited or the context of the study area  
417 restricts the implementation of some strategies, implementing even a single strategy can still  
418 help to reduce CT theft. Nevertheless, we suggest that the implementation of these strategies  
419 should be accompanied by careful consideration of the potential trade-offs they might have  
420 for data quality and sampling regimes.

421

422 **Acknowledgements**

423 We would like to thank the members of the Dynamics of Eco-Evolutionary Patterns  
424 (D.E.E.P.) research group at the University of Tasmania. Animal ethics permit was obtained  
425 prior to this study through the University of Tasmania Animal Ethics Committee (number  
426 FA20109). A human ethics exemption was obtained prior to this study through the University

427 of Tasmania Human Ethics Committee (number H83639). Funding provided by the  
428 Australian Research Council Funding (FL160100101) to BWB.

429

430 **Conflict of interest statement**

431 The authors declare no conflict of interest.

432

433

434

435

436

437

438

439

440

441

442

443

444

445

446



447 **References**

- 448 Abdu, N.H. 2023. The problem of illegal wood harvesting in Tasmania: an analysis of the institutional  
449 setting and the potential for a labelling system. University of Tasmania.  
450 <https://doi.org/10.25959/100.00047571>.
- 451 Barclay, E. ,Donnermeyer, J.F. 2011. Crime and security on agricultural operations. *Security Journal*,  
452 24, 1-18. <https://doi.org/10.1057/sj.2008.23>.
- 453 Beery, S., Morris, D. ,Yang, S. 2019. Efficient Pipeline for Camera Trap Image Review. *arXiv preprint*.  
454 <https://doi.org/10.48550/arXiv.1907.06772>.
- 455 Brilleman, S., Elci, E., Buros, J. ,Wolfe, R. 2020. Bayesian Survival Analysis Using the rstanarm R  
456 Package. *arXiv preprint*. <https://doi.org/10.48550/arXiv.2002.09633>.
- 457 Brook, B.W., Buettel, J.C. ,Aandahl, R.Z. 2023. A user-friendly AI workflow for customised wildlife-  
458 image classification. *EcoEvoRxiv preprint*. <https://doi.org/10.32942/X2ZW3D>.
- 459 Burns, P.A., Parrott, M.L., Rowe, K.C. ,Phillips, B.L. 2018. Identification of threatened rodent species  
460 using infrared and white-flash camera traps. *Australian Mammalogy*, 40, 188-197.  
461 <https://doi.org/10.1071/AM17016>.
- 462 Burton, A.C., Neilson, E., Moreira, D., Ladle, A., Steenweg, R., Fisher, J.T., Bayne, E. ,Boutin, S. 2015.  
463 REVIEW: Wildlife camera trapping: a review and recommendations for linking surveys to  
464 ecological processes. *Journal of Applied Ecology*, 52, 675-685. [https://doi.org/10.1111/1365-](https://doi.org/10.1111/1365-2664.12432)  
465 [2664.12432](https://doi.org/10.1111/1365-2664.12432).
- 466 Cardona, L.M., Brook, B.W., Harwood, A. ,Buettel, J.C. 2024. Measuring the human-dimension of  
467 outdoor recreation and its impacts on terrestrial wildlife. *Journal of Outdoor Recreation and*  
468 *Tourism*, 47, 100808. <https://doi.org/10.1016/j.jort.2024.100808>.
- 469 Clarin, B.M., Bitzilekis, E., Siemers, B.M. ,Goerlitz, H.R. 2014. Personal messages reduce vandalism  
470 and theft of unattended scientific equipment. *Methods in Ecology and Evolution*, 5, 125-131.  
471 <https://doi.org/10.1111/2041-210X.12132>.

472 Clements, G.R., Lynam, A.J., Gaveau, D., Yap, W.L., Lhota, S., Goosem, M., Laurance, S., Laurance, W.F.  
473 2014. Where and How Are Roads Endangering Mammals in Southeast Asia's Forests? *PLoS*  
474 *ONE*, 9, e115376. <https://doi.org/10.1371/journal.pone.0115376>.

475 Cusack, J.J., Dickman, A.J., Rowcliffe, J.M., Carbone, C., Macdonald, D.W., Coulson, T. 2015. Random  
476 versus Game Trail-Based Camera Trap Placement Strategy for Monitoring Terrestrial Mammal  
477 Communities. *PLoS ONE*, 10, e0126373. <https://doi.org/10.1371/journal.pone.0126373>.

478 Donders, A.R.T., van der Heijden, G.J.M.G., Stijnen, T., Moons, K.G.M. 2006. Review: A gentle  
479 introduction to imputation of missing values. *Journal of Clinical Epidemiology*, 59, 1087-1091.  
480 <https://doi.org/10.1016/j.iclinepi.2006.01.014>.

481 George, S.L., Crooks, K.R. 2006. Recreation and large mammal activity in an urban nature reserve.  
482 *Biological Conservation*, 133, 107-117. <https://doi.org/10.1016/j.biocon.2006.05.024>.

483 Gerben J. N. Bruinsma 2007. Urbanization and Urban Crime: Dutch Geographical and Environmental  
484 Research. *Crime and Justice*, 35, 453-502. <https://doi.org/10.1086/650190>.

485 Glen, A.S., Cockburn, S., Nichols, M., Ekanayake, J., Warburton, B. 2013. Optimising Camera Traps for  
486 Monitoring Small Mammals. *PLoS ONE*, 8, e67940.  
487 <https://doi.org/10.1371/journal.pone.0067940>.

488 Glover-Kapfer, P., Soto-Navarro, C.A., Wearn, O.R. 2019. Camera-trapping version 3.0: current  
489 constraints and future priorities for development. *Remote Sensing in Ecology and*  
490 *Conservation*, 5, 209-223. <https://doi.org/10.1002/rse2.106>.

491 Hossain, A.N.M., Barlow, A., Barlow, C.G., Lynam, A.J., Chakma, S., Savini, T. 2016. Assessing the  
492 efficacy of camera trapping as a tool for increasing detection rates of wildlife crime in tropical  
493 protected areas. *Biological Conservation*, 201, 314-319.  
494 <https://doi.org/10.1016/j.biocon.2016.07.023>.

495 Iannarilli, F., Erb, J., Arnold, T.W., Fieberg, J.R. 2021. Evaluating species-specific responses to camera-  
496 trap survey designs. *Wildlife Biology*, 2021, 1-12. <https://doi.org/10.2981/wlb.00726>.

497 Karanth, K.U., Nichols, J.D., Kumar, N.S., Hines, J.E. 2006. Assessing tiger population dynamics using  
498 photographic capture-recapture sampling. *Ecology*, 87, 2925-2937.  
499 [https://doi.org/10.1890/0012-9658\(2006\)87\[2925:ATPDUP\]2.0.CO;2](https://doi.org/10.1890/0012-9658(2006)87[2925:ATPDUP]2.0.CO;2).

500 Kassambara, A., Kosinski, M., Biecek, P., Fabian, S. 2021. survminer: drawing survival curves using  
501 'ggplot2'. R package v0.4.9. <https://doi.org/10.32614/CRAN.package.survminer>.

502 Kelly, M.J., Holub, E.L. 2008. Camera Trapping of Carnivores: Trap Success Among Camera Types and  
503 Across Species, and Habitat Selection by Species, on Salt Pond Mountain, Giles County,  
504 Virginia. *Northeastern Naturalist*, 15, 249-262. [https://doi.org/10.1656/1092-  
505 6194\(2008\)15\[249:CTOCTS\]2.0.CO;2](https://doi.org/10.1656/1092-6194(2008)15[249:CTOCTS]2.0.CO;2).

506 Kukielka, E., Barasona, J.A., Cowie, C.E., Drewe, J.A., Gortazar, C., Cotarelo, I., Vicente, J. 2013. Spatial  
507 and temporal interactions between livestock and wildlife in South Central Spain assessed by  
508 camera traps. *Preventive Veterinary Medicine*, 112, 213-221.  
509 <https://doi.org/10.1016/j.prevetmed.2013.08.008>.

510 Lin, X., Cai, B., Wang, L., Zhang, Z. 2015. A Bayesian proportional hazards model for general interval-  
511 censored data. *Lifetime Data Analysis*, 21, 470-490. [https://doi.org/10.1007/s10985-014-  
512 9305-9](https://doi.org/10.1007/s10985-014-9305-9).

513 Mackenzie, C., Hartter, J. 2013. Demand and proximity: Drivers of illegal forest resource extraction.  
514 *ORYX*, 47, 288-297. <https://doi.org/10.1017/S0030605312000026>.

515 Mann, G.K.H., O'Riain, M.J., Parker, D.M. 2015. The road less travelled: assessing variation in  
516 mammal detection probabilities with camera traps in a semi-arid biodiversity hotspot.  
517 *Biodiversity and Conservation*, 24, 531-545. <https://doi.org/10.1007/s10531-014-0834-z>.

518 Meek, P.D., Ballard, G., Claridge, A., Kays, R., Moseby, K., O'Brien, T., O'Connell, A., Sanderson, J.,  
519 Swann, D.E., Tobler, M., Townsend, S. 2014. Recommended guiding principles for reporting  
520 on camera trapping research. *Biodiversity and Conservation*, 23, 2321-2343.  
521 <https://doi.org/10.1007/s10531-014-0712-8>.

522 Meek, P.D., Ballard, G.A., Fleming, P.J.S. 2012a. A permanent security post for camera trapping.  
523 *Australian Mammalogy*, 35, 123-127. <https://doi.org/10.1071/AM12014>.

524 Meek, P.D., Ballard, G.A., Sparkes, J., Robinson, M., Nesbitt, B., Fleming, P.J.S. 2019. Camera trap theft  
525 and vandalism: occurrence, cost, prevention and implications for wildlife research and  
526 management. *Remote Sensing in Ecology and Conservation*, 5, 160-168.  
527 <https://doi.org/10.1002/rse2.96>.

528 Meek, P.D., Pittet, A. 2012b. User-based design specifications for the ultimate camera trap for wildlife  
529 research. *Wildlife Research*, 39, 649-660. <https://doi.org/10.1071/WR12138>.

530 Meek, P.D., Vernes, K. 2015. Can camera trapping be used to accurately survey and monitor the  
531 Hastings River mouse (*Pseudomys oralis*)? *Australian Mammalogy*, 38, 44-51.  
532 <https://doi.org/10.1071/AM15016>.

533 Miller, A.B., Leung, Y.-F., Kays, R. 2017. Coupling visitor and wildlife monitoring in protected areas  
534 using camera traps. *Journal of Outdoor Recreation and Tourism*, 17, 44-53.  
535 <https://doi.org/10.1016/j.jort.2016.09.007>.

536 Moll, R.J., Ortiz-Calo, W., Cepek, J.D., Lorch, P.D., Dennis, P.M., Robison, T., Montgomery, R.A. 2020.  
537 The effect of camera-trap viewshed obstruction on wildlife detection: implications for  
538 inference. *Wildlife Research*, 47, 158-165. <https://doi.org/10.1071/WR19004>.

539 Nakagawa, S., Freckleton, R.P. 2011. Model averaging, missing data and multiple imputation: a case  
540 study for behavioural ecology. *Behavioral Ecology and Sociobiology*, 65, 103-116.  
541 <https://doi.org/10.1007/s00265-010-1044-7>.

542 Pan, C., Cai, B., Wang, L. 2020. A Bayesian approach for analyzing partly interval-censored data under  
543 the proportional hazards model. *Statistical Methods in Medical Research*, 29, 3192-3204.  
544 <https://doi.org/10.1177/0962280220921552>.

545 Paton, A.J., Brook, B.W., Buettel, J.C. 2024. A non-invasive approach to measuring body dimensions of  
546 wildlife with camera traps: A felid field trial. *Ecology and Evolution*, 14, e11612.  
547 <https://doi.org/10.1002/ece3.11612>.

548 Paula, J.J.S., Bispo, R.M.B., Leite, A.H., Pereira, P.G.S., Costa, H.M.R.G., Fonseca, C.M.M.S.,  
549 Mascarenhas, M.R.T., Bernardino, J.L.V. 2015. Camera-trapping as a methodology to assess  
550 the persistence of wildlife carcasses resulting from collisions with human-made structures.  
551 *Wildlife Research*, 41, 717-725. <https://doi.org/10.1071/WR14063>.

552 Pyšková, K., Kauzál, O., Storch, D., Horáček, I., Pergl, J., Pyšek, P. 2018. Carnivore distribution across  
553 habitats in a central-European landscape: a camera trap study. *Zookeys*, 227-246.  
554 <https://doi.org/10.3897/zookeys.770.22554>.

555 R Core Team 2020. R: A language and environment for statistical computing. R Foundation for  
556 Statistical Computing.

557 Rovero, F., Marshall, A.R. 2009. Camera trapping photographic rate as an index of density in forest  
558 ungulates. *Journal of Applied Ecology*, 46, 1011-1017. [https://doi.org/10.1111/j.1365-  
559 2664.2009.01705.x](https://doi.org/10.1111/j.1365-2664.2009.01705.x).

560 Sidebottom, A., Tompson, L., Thornton, A., Bullock, K., Tilley, N., Bowers, K., Johnson, S.D. 2018.  
561 Gating Alleys to Reduce Crime: A Meta-Analysis and Realist Synthesis. *Justice Quarterly*, 35,  
562 55-86. <https://doi.org/10.1080/07418825.2017.1293135>.

563 Tanwar, K.S., Sadhu, A., Jhala, Y.V. 2021. Camera trap placement for evaluating species richness,  
564 abundance, and activity. *Scientific Reports*, 11, 23050. [https://doi.org/10.1038/s41598-021-  
565 02459-w](https://doi.org/10.1038/s41598-021-02459-w).

566 Taylor, J.C., Bates, S.B., Whiting, J.C., McMillan, B.R., Larsen, R.T. 2022. Using camera traps to estimate  
567 ungulate abundance: a comparison of mark–resight methods. *Remote Sensing in Ecology and  
568 Conservation*, 8, 32-44. <https://doi.org/10.1002/rse2.226>.

569 Therneau, T.M. 2020. Coxme: mixed effects cox models. R package v2.2-16.  
570 <https://doi.org/10.32614/CRAN.package.coxme>.

571 Troy, A., Morgan Grove, J., O’Neil-Dunne, J. 2012. The relationship between tree canopy and crime  
572 rates across an urban–rural gradient in the greater Baltimore region. *Landscape and Urban  
573 Planning*, 106, 262-270. <https://doi.org/10.1016/j.landurbplan.2012.03.010>.

574 van de Schoot, R., Depaoli, S., King, R., Kramer, B., Märtens, K., Tadesse, M.G., Vannucci, M., Gelman,  
575 A., Veen, D., Willemsen, J., Yau, C. 2021. Bayesian statistics and modelling. *Nature Reviews*  
576 *Methods Primers*, 1, 1. <https://doi.org/10.1038/s43586-020-00001-2>.

577 Vaughan, P.M., Buettel, J.C., Brook, B.W. 2022. Investigating Avian Behaviour Using Opportunistic  
578 Camera-Trap Imagery Reveals an Untapped Data Source. *Ornithological Science*, 21, 3-12.  
579 <https://doi.org/10.2326/osj.21.3>.

580 Wegge, P., Pokheral, C.P., Jnawali, S.R. 2004. Effects of trapping effort and trap shyness on estimates  
581 of tiger abundance from camera trap studies. *Animal Conservation*, 7, 251-256.  
582 <https://doi.org/10.1017/S1367943004001441>.  
583 <https://www.cambridge.org/core/product/3584B5AED9CF8467CF866B7DECE4957B>.

584 Woods, W.E. 2019. A political ecology study of forest wilderness in the Olympic Peninsula (USA) and  
585 Tasmania (Australia). The University of Queensland. <https://doi.org/10.14264/uql.2020.77>.

586 Yates, L.A., Aandahl, Z., Richards, S.A., Brook, B.W. 2023. Cross validation for model selection: A  
587 review with examples from ecology. *Ecological Monographs*, 93, e1557.  
588 <https://doi.org/10.1002/ecm.1557>.

589 Zahoor, B., Liu, X., Ahmad, B. 2023. Activity patterns of Asiatic black bear (*Ursus thibetanus*) in the  
590 moist temperate forests of Machiara National Park, Azad Jammu and Kashmir, Pakistan.  
591 *Environmental Science and Pollution Research*, 30, 8036-8047.  
592 <https://doi.org/10.1007/s11356-022-22646-0>.

593

594

595

596

597

598

599

600

601